



Deep oxidative desulfurization of simulated and real gas oils by $\text{NiFe}_2\text{O}_4@\text{SiO}_2\text{-DETA@POM}$ as a retrievable hybrid nanocatalyst

Mohammad Ali Bodaghifard^{1,2} · Mahdia Hamidinasab² · Pegah Bayat¹

Received: 13 January 2023 / Accepted: 19 March 2023 / Published online: 27 March 2023
© The Author(s), under exclusive licence to Springer-Verlag GmbH Germany, part of Springer Nature 2023

Abstract

Magnetic nanoparticles surrounded with a silica shell are useful materials to immobilize active agents on their surface. Here, a heteropolyacid-functionalized hybrid nanomaterial ($\text{NiFe}_2\text{O}_4@\text{SiO}_2\text{-DETA@POM}$) was prepared and characterized by X-ray powder diffraction patterns (XRD), Fourier-transform infrared spectroscopy (FT-IR), thermogravimetric analysis (TGA/DTG), vibrating sample magnetometer (VSM), the field emission scanning electron microscopy (FE-SEM), and the electron-dispersive X-ray spectroscopy (EDS). The synthesized hybrid nanostructure was used as a solid nanocatalyst in oxidative desulfurization (ODS) of real fuel and simulated gasoline samples. The ODS process of benzothiophene (BT) and dibenzothiophene (DBT) as model compounds in the presence of $\text{NiFe}_2\text{O}_4@\text{SiO}_2\text{-DETA@POM}$ and by using urea-hydrogen peroxide/acetic acid as a safer oxidizing agent was investigated. A good result was obtained by removing 97% of benzothiophene and 98% of dibenzothiophene. Also, 96% of the sulfur compounds were eliminated when the ODS process was tested on a real crude oil sample (600 ppm) under an optimized dosage of nanocatalyst, urea-hydrogen peroxide/acetic acid (0.1 g, 1 g/4 ml) at 50 °C for 60 min. $\text{NiFe}_2\text{O}_4@\text{SiO}_2\text{-DETA@POM}$ could be recycled for five consecutive oxidation runs without significant deterioration in its catalytic activity. The UHP's safety and efficiency as an oxidant, high removal efficacy, short transformation times, easy workup procedure, catalyst reusability, simple separation of nanocatalyst, green conditions, and environmental compatibility and sustainability. The obtained results prove that $\text{NiFe}_2\text{O}_4@\text{SiO}_2\text{-DETA@POM}$ is a suitable and efficient hybrid catalyst for the oxidative desulfurization of simulated and real fuels.

Keywords Environment · Oxidative desulfurization (ODS) · Heteropolyacid (HPA) · Magnetic nanoparticles · Hybrid nanomaterials

Introduction

Sulfur exists in both organic and inorganic forms in fossil fuels. The harmful SO_x gases emitted during fuel combustion led to the pollution of the atmosphere. Due to the high toxicity, corrosive nature, serious environmental problems, and human health risks of sulfur-containing impurities, the main concern in the refinery industry has been the production of fuels with an ultra-low level of sulfur content (Rezvani and Imani 2021). The

sulfur content of fuels is removed conventionally by hydrodesulfurization (HDS). Dibenzothiophene (DBT) as a polyaromatic organosulfur compound and similar derivatives indicates lower activity in the hydrodesulfurization process (Rezvani and Fereyduni 2019). As a result, the HDS process operated under elevated pressures and temperatures to attain deep desulfurization, which increases the process cost. Due to the drawbacks of HDS, alternative desulfurization techniques such as adsorption desulfurization (ADS) (Yang et al. 2018), extraction desulfurization (EDS) (Jiang et al. 2016), bio-desulfurization (Boniek et al. 2015), ultrasound-assisted oxidation (Chen et al. 2010), and oxidative desulfurization (ODS) (Gu et al. 2017; Liu et al. 2020; Chen et al. 2010; Safa et al. 2017; Rezvani et al. 2018, Rezvani et al. 2020a; Rezvani and Fereyduni 2019; Rezvani and Imani 2021) have been considered and developed. Among them, oxidative desulfurization (ODS) should be the most promising method due to its high desulfurization efficiency [17–21]. In the ODS procedure, the sulfur-containing compounds are oxidized

Responsible Editor: George Z. Kyzas

✉ Mohammad Ali Bodaghifard
mbodaghi2007@yahoo.com; m-bodaghifard@araku.ac.ir

¹ Department of Chemistry, Faculty of Science, Arak University, Arak 38156-88138, Iran

² Institute of Nanosciences and Nanotechnology, Arak University, Arak 38156-88138, Iran

to corresponding sulfides or sulfones in the presence of active oxygen species. The oxidized products can be removed or extracted by a polar solvent. Oxidative desulfurization (ODS) is thoroughly studied and performed under atmospheric pressure at room temperature. So, the mild operating conditions of this method make it an economical technique for the removal of organosulfur compounds from fuels (Boniek et al. 2015). However, there is still demand for designing more efficient heterogeneous catalysts for use in the ODS process. Polyoxometalates (POMs) are inorganic clusters between oxygen and tens to hundreds of early transition metal atoms (e.g., $M=V, Mo, W, Ti$), and different types of heteroatoms (e.g., $X=P, As, Si, Ge$) can be found in their structure (Zhou et al. 2014). POMs have a large variety of compositions and sizes that find various applications in medicine, catalysis, and materials chemistry (Zhou et al. 2014). A specific number of electrons can be accepted or released by POMs without changing or decomposition in their structural frameworks, which makes them good candidates in electrocatalysis and redox chemistry (Ammam 2013). To overcome the self-aggregation, tedious separation, decreasing the catalytic activity of POMs, and requirement of sustainable processes, numerous researchers have considered the supporting of POMs on different solid materials to access heterogeneous catalysts (Ye and Wu 2016). Many effective methods have been developed to heterogeneity and immobilize the POMs, including encapsulation, intercalation, electrodeposition, impregnation, chemisorption, co-condensation sol–gel methods, hydrothermal, solvothermal, and the covalent grafting of POMs into the surface of various solid supports (Cherevan et al. 2020). Many research groups described the stabilization of POMs on different kinds of solid supports and their catalytic applications in organic synthesis, hydrolysis, photocatalysis, electrocatalysis, oxidation, and oxidative desulfurization that benefit from high selectivity and easy workup procedure (Jiang et al. 2016; Liu et al. 2020; Ye and Wu 2016; Craven et al. 2018; Rezvani and Fereyduni 2019; Cherevan et al. 2020; Rezvani et al. 2020b; Rezvani and Mirsadri 2020; Taghizadeh et al. 2020; Rezvani and Imani 2021). Magnetic nanoparticles (MNPs) do not have tedious separation procedures and are separated easily by a magnet. Besides, they have a high surface area for catalytic application (Injumba et al. 2017). Coating the MNPs with a polymeric or inorganic matrix reduced their undesirable features such as aggregation and leaching under acidic conditions (Hozhabr Araghi and Entezari 2015). SiO_2 has high chemical-thermal stability and can be modified by many kinds of functional groups. So, SiO_2 is a suitable coating agent to increase the chemical and colloidal stability of MNPs (Gawande et al. 2013; Bodaghifard et al. 2018). As part of our ongoing endeavor to extend green organic reactions and efficient heterogeneous magnetic nanocatalysts (Bodaghifard 2019; Hamidinasab et al. 2020a; Bodaghifard and Shafi 2021), a new heterogeneous polyoxometalate-supported hybrid nanostructure was fabricated [MNPs@ SiO_2 -DETA@POM]. In this work, POM was immobilized on $NiFe_2O_4$ @ SiO_2 surface to act

as an efficient heterogeneous nanocatalyst for the oxidative desulfurization process of diesel fuel. The thiophenic sulfur compounds (benzothiophene and dibenzothiophene) were dissolved in *n*-heptane to access a simulated fuel. Then, the catalytic proficiency of prepared hybrid nanomaterial [MNPs@ SiO_2 -DETA@POM] on the ODS of typical and real gasoline was investigated. The prepared hybrid catalyst showed high catalytic activity in the oxidation of sulfur compounds. In addition, the catalyst could be reused easily due to its fast magnetic separation.

Experimental

All chemical materials were purchased from reputable chemical companies (Merck, Across, Sigma-Aldrich) and were used without further purification. Urea-hydrogen peroxide was prepared in the laboratory. The real crude oil sample was supplied by the South Pars Company (Iran). The crystal structure was carried out by Philips XPERT X-ray powder diffraction (XRD) diffractometer (Cu-K α radiation and $\lambda=0.15406$) in the range of Bragg angle 10–80 using 0.05° as the step length. The FT-IR spectra were recorded by Unicom Galaxy Series. The surface morphology and elemental content of MNPs@ SiO_2 -DETA@POM were investigated on a Hitachi S-4160. The thermal stability of MNPs@ SiO_2 -DETA@POM was investigated by a thermogravimetric analyzer with model Mettler TA4000 System under an N_2 atmosphere at a heating rate of $10^\circ C min^{-1}$. The magnetization and hysteresis loop for the synthesized magnetic nanoparticles were measured at room temperature using a 7300 VSM system with a maximum field of 10 kOe. The content of total sulfur in gasoline and model fuel was measured by an X-ray sulfur analyzer (Tanaca spectrometer RX 360 SH) using X-ray fluorescence (XRF) technique.

Preparation of nano- $NiFe_2O_4$ @ SiO_2 -DETA

The co-preparation method was applied to prepare the magnetic nickel-ferrite nanoparticles (Hamidinasab et al. 2020b). Hydrolysis of TEOS in a basic solution leads to the formation of a silica shell onto the $NiFe_2O_4$ nanoparticles surface (Ahadi et al. 2020). The reaction of nano- $NiFe_2O_4$ @ SiO_2 with 3-chloropropyltrimethoxysilane produced the nano- $NiFe_2O_4$ @ SiO_2 -PrCl particles [32]. 0.5 g $NiFe_2O_4$ @ SiO_2 -PrCl was mixed with 25 mL dry toluene and sonicated for 30 min. Then 5.53 mmol (0.06 mL) of diethylenetriamine was added, and the suspension was heated at $80^\circ C$ for 24 h. The $NiFe_2O_4$ @ SiO_2 -DETA was separated by a magnet, eluted with toluene, and dried in an oven ($80^\circ C$).

Preparation of nano- $NiFe_2O_4$ @ SiO_2 -DETA@POM

The $NiFe_2O_4$ @ SiO_2 -DETA (0.3 g) was dispersed in deionized water (50 mL) for 30 min, then the solution of $H_4PMo_{11}TiO_{40}$

(0.7 g in 20 mL deionized water) was appended to the suspension (30 °C). The suspension was mixed at room temperature for 24 h. The $\text{NiFe}_2\text{O}_4@ \text{SiO}_2\text{-DEA@POM}$ was isolated by a magnet, rinsed with deionized water ($3 \times 10 \text{ mL}$), and dried in an oven (60 °C).

Batch ODS experiment of simulated gas oil and real gas oil

At first, 600 ppm of the sulfur content solution was prepared with the proper amount of model compounds (BT and DBT) in n-heptane (25 mL). Then 0.1 g of urea-hydrogen peroxide/acetic acid (1 g/4 mL), 0.1 g of $\text{NiFe}_2\text{O}_4@ \text{SiO}_2\text{-DETA@POM}$ as a nanocatalyst, and 25 mL of the simulated or real fuel solution was added into the round bottom flask at 50 °C under ultrasound condition for 60 min. After completing the reaction, the solution was cooled to room temperature, and by using an external magnet the magnetic nanocatalyst was separated. Then, 4 mL of polar acetonitrile was poured to extract products of the oxidation process. A separation funnel was used to separate the immiscible mixture of n-heptane and water phase.

Result and discussion

Preparation and characterization of the hybrid nanostructure

Polyoxometalate-organic molecule tags were grafted onto the surface of nickel-ferrite nanoparticles to afford a new heterogeneous magnetic nanocatalyst. Scheme 1 shows the schematic steps for the preparation of $\text{MNPs}@ \text{SiO}_2\text{-DETA@POM}$ nanostructure. FT-IR spectroscopy, FE-SEM, TEM, XRD patterns, EDS, EDS map scan, VSM, and TGA

as standard techniques were used to characterize the prepared nanostructure.

The FT-IR spectra of bare NiFe_2O_4 MNPs, $\text{NiFe}_2\text{O}_4@ \text{SiO}_2$ MNPs, $\text{NiFe}_2\text{O}_4@ \text{SiO}_2\text{-PrCl}$, $\text{NiFe}_2\text{O}_4@ \text{SiO}_2\text{-DETA}$, and $\text{NiFe}_2\text{O}_4@ \text{SiO}_2\text{-DETA@POM}$ was recorded in the range of 400–4000 cm^{-1} (Fig. 1). Strong absorption bands around 422 and 591 cm^{-1} , corresponding to stretching vibration of Ni–O and Fe–O sites, are seen in the curve (a) (Sen et al. 2015). The formation of a silica layer was confirmed by the appearance of the absorption at 468 cm^{-1} , 959 cm^{-1} , 801 cm^{-1} , and 1086 cm^{-1} , that related to symmetric and asymmetric stretching vibration bands of Si–O–Si groups (curve b). H–O–H molecules adsorbed on the silica surface show a weak twisting vibration band at 1628 cm^{-1} . The weak aliphatic C–H symmetric and asymmetric stretching vibrations at 2930 and 2984 cm^{-1} confirmed the anchoring of alkyl groups (curves c to e). The NH bending and C–N stretching bands appeared at 1632 and 1384 cm^{-1} in

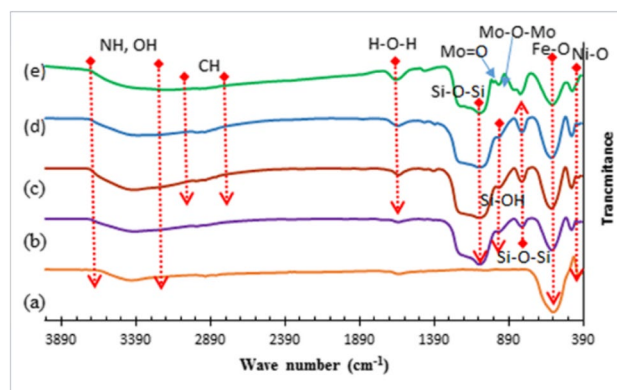
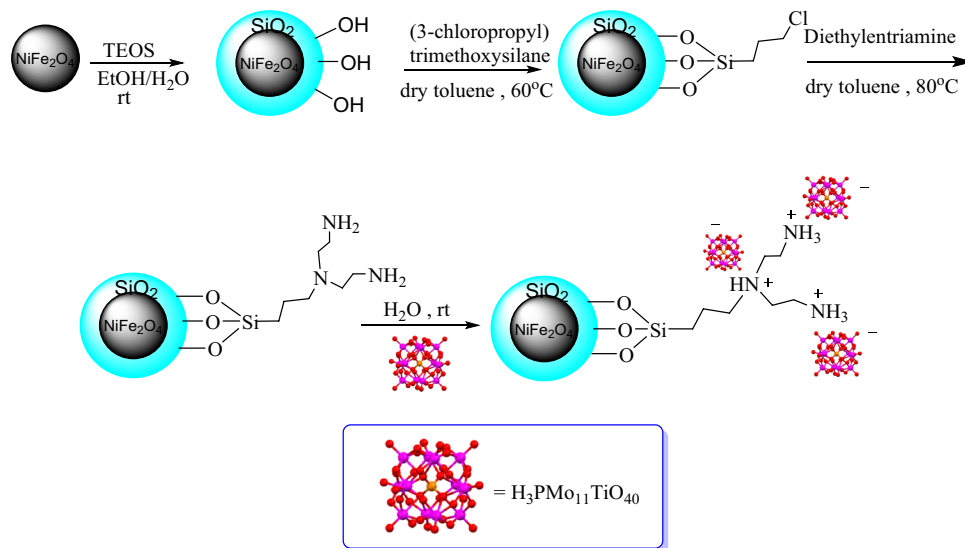


Fig. 1 The FT-IR spectra of **a** NiFe_2O_4 , **b** $\text{NiFe}_2\text{O}_4@ \text{SiO}_2$, **c** $\text{NiFe}_2\text{O}_4@ \text{SiO}_2\text{-PrCl}$, **d** $\text{NiFe}_2\text{O}_4@ \text{SiO}_2\text{-DETA}$, and **e** $\text{NiFe}_2\text{O}_4@ \text{SiO}_2\text{-DETA@POM}$

Scheme 1 Preparation of polyoxometalate-supported hybrid nanostructure ($\text{MNPs}@ \text{SiO}_2\text{-DETA@POM}$)



curves d and e. The bands observed in the range of 3200 to 3500 cm^{-1} correspond to the stretching vibration of N–H and OH groups. The stretching vibration of Mo–O–Mo and Mo=O in curve e appeared at 992 and 1000 cm^{-1} , respectively. The P–O vibration appears at 1080 cm^{-1} , which overlaps with the Si–O band (curve e). Figure 2 shows the FT-IR spectra of NiFe_2O_4 @ SiO_2 -DEA (a), NiFe_2O_4 @ SiO_2 -DEA@POM (b), and heteropolyacid (HPA) which indicate POM (HPA) grafted successfully on the surface of NiFe_2O_4 @ SiO_2 -DETA particles.

Figure 3 shows X-ray patterns of NiFe_2O_4 nanoparticles and NiFe_2O_4 @ SiO_2 -DETA@POM particles. Many diffraction peaks at (111), (220), (311), (222), (400), (422), (511), (440), and (533) Miller planes appeared and confirmed that the crystal structure of NiFe_2O_4 nanoparticles is cubic (Nejati and Zabihi 2012; Kim et al. 2014), which comply with standard JCPDS file (no. 44–1485) (Sen et al. 2015). Figure 6b shows 5 specific peaks in $2\theta = 12.7, 23.3, 25.7, 29.7, 38.9$ that related to the MoO_3 bonds in heteropolyacid structure. The Scherrer equation ($D = K\lambda/\beta\cos\theta$) was applied for the estimation of the average crystallite size of NiFe_2O_4 @ SiO_2 -DETA@POM. λ is the x-ray Cu wavelength, β is the width of the x-ray peak on the 2θ axis, which is measured as the line broadening at half the maximum intensity, θ is the Bragg angle, and K is the so-called Scherrer constant. The average crystallite size as calculated from the width of the peak at $2\theta = 35.8^\circ$ (311), is 23 nm, which is smaller than the range determined using FE-SEM and TEM analyses (Figs. 4 and 5).

Figure 4 shows the FE-SEM image of the hybrid nanostructure. In Fig. 4a, the spherical and regular shape of NiFe_2O_4 @ SiO_2 -DETA@POM nanoparticles is visible. The histogram chart in Fig. 4b shows 45 nm mean diameter for the nanoparticles. The nanoparticles' morphology, shape, and size were elucidated by transmission electron microscopy (Fig. 5). The TEM analysis revealed that NiFe_2O_4 @

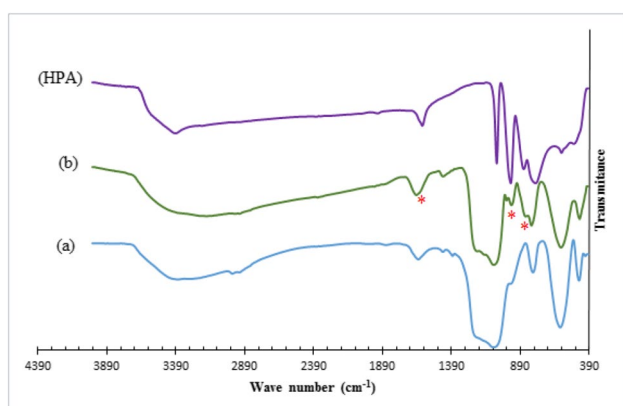


Fig. 2 The FT-IR spectra of NiFe_2O_4 @ SiO_2 -DEA (a), NiFe_2O_4 @ SiO_2 -DETA@POM (b), and heteropolyacid (HPA)

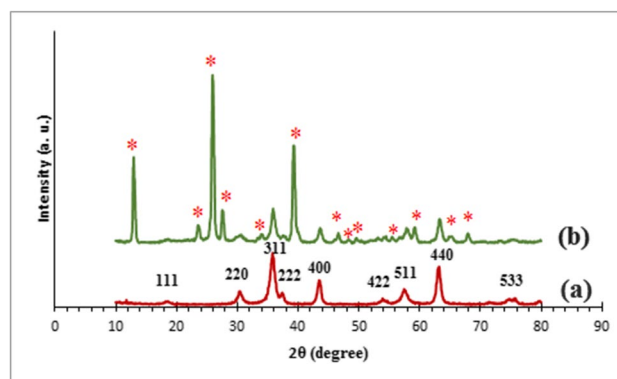


Fig. 3 The XRD patterns of **a** NiFe_2O_4 nanoparticles and **b** NiFe_2O_4 @ SiO_2 -DETA@POM particles

SiO_2 -DETA@POM magnetic nanoparticles have almost spherical shapes, and average particles size was detected as 30–60 nm.

The energy dispersive X-ray spectroscopy (EDS) of NiFe_2O_4 @ SiO_2 -DETA@POM particles shows the existence of Fe, Ni, Si, P, Mo, N, and C atoms (Fig. 6). The EDS map scan indicates that the elements are well dispersed on the surface of the hybrid nanostructure (Fig. 7). These results corroborate the prosperous construction of NiFe_2O_4 @ SiO_2 -DETA@POM nanomaterial.

The magnetic properties of NiFe_2O_4 and NiFe_2O_4 @ SiO_2 -DETA@POM nanoparticles were elucidated using a vibrating sample magnetometer (VSM) at room temperature (Fig. 8a and b). The S-like magnetization curves, the coincidence of the hysteresis loop (H_c), the low remanence (M_r), and the coercivity confirm the superparamagnetic behaviors of these hybrid materials. The magnetization of the sample could be completely saturated at high fields. M_s of the sample was dropped from 21.2 to 10.3 emu g^{-1} due to the formation of core/shell nanostructure.

The stability of NiFe_2O_4 @ SiO_2 -DETA@POM nanocatalyst was evaluated using TGA/DTG technique (Fig. 9). The initial 2% weight loss from r.t. to about 190 $^\circ\text{C}$ is related to the elimination of water and solvent molecules that are physically adsorbed and hydroxyl groups located on the surface of nanostructure. The decomposition of the organic tags within the nanostructure makes the major weight loss (8%W) beyond 190 $^\circ\text{C}$ to nearly 800 $^\circ\text{C}$. Therefore, the catalyst shows good thermal stability and can be used safely under heterogeneous conditions.

Oxidation desulfurization of simulated fuels

After the characterization of NiFe_2O_4 @ SiO_2 -DETA@POM nanostructure, its effect on the removal of sulfur contaminants was investigated on the model fuel. In this work, during the oxidation-desulfurization (ODS) process,

Fig. 4 The FE-SEM image (a) and histogram chart (b) of NiFe₂O₄@SiO₂-DETA@POM

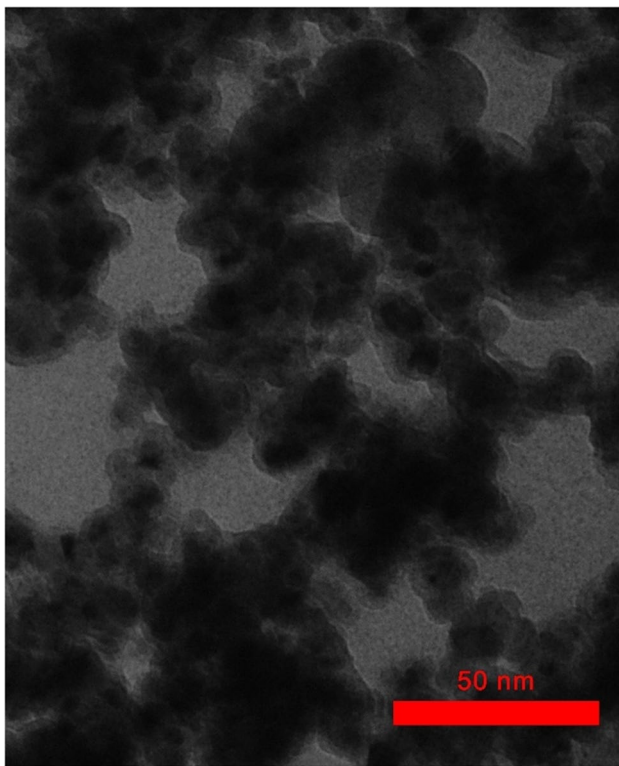
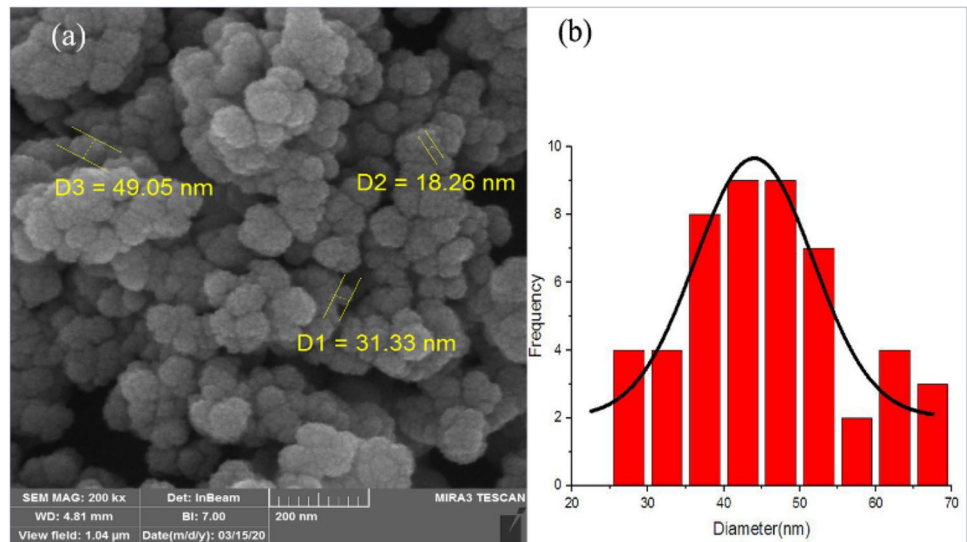


Fig. 5 The TEM image of NiFe₂O₄@SiO₂-DETA@POM

the urea-H₂O₂ was used as a safe oxidant accompanying acetic acid to in situ forming of active per-acid. This oxidation system can efficiently transform organic sulfurs into sulfoxide and sulfone compounds without producing residual products. Benzothiophene (BT) and dibenzothiophene (DBT) as sources of sulfur solution (600 ppm) were mixed

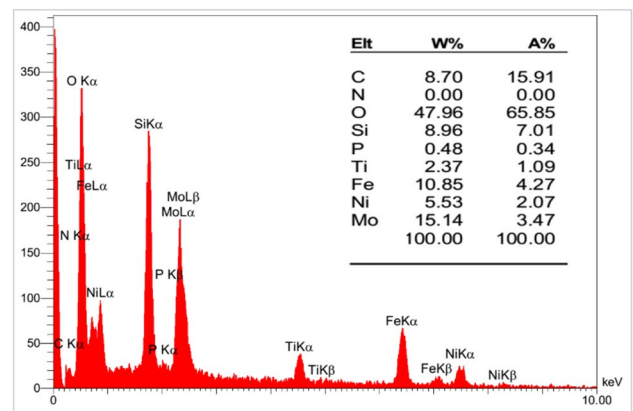


Fig. 6 EDS spectrum of nano-NiFe₂O₄@SiO₂-DETA@POM particles

with urea-hydrogen peroxide/acetic acid and NiFe₂O₄@SiO₂-DETA@POM as a catalyst then the oxidation reaction was carried out at 50 °C under ultrasound condition. Extraction of oxidized compounds was done using a polar liquid (acetonitrile) to obtain a sample with low sulfur content. The following equation was afforded the percentage of sulfur removal ($\Delta S\%$):

$$\Delta S(\%) = \left[\frac{S_i - S_f}{S_i} \right] \times 100$$

where S_i represents the initial concentration and S_f is the final concentration of sulfur compounds (ppm), respectively. The XRF technique was applied to analyze the sulfur content. At a controlled temperature and time, the amount of nanocatalyst and oxidizer was optimized, and following that, the temperature and time were optimized.

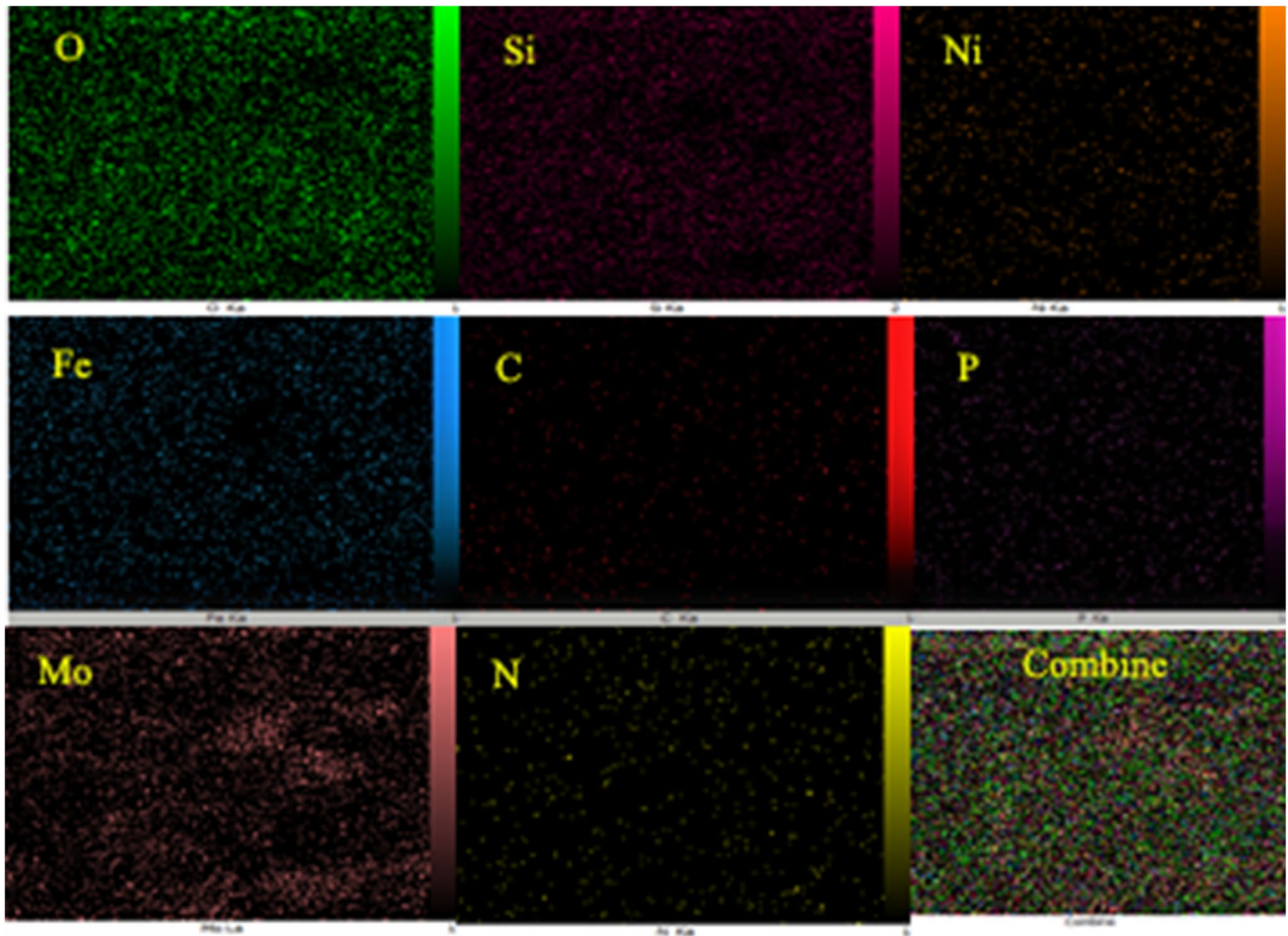


Fig. 7 EDS map scan of $\text{NiFe}_2\text{O}_4@\text{SiO}_2\text{-DETA@POM}$ particles

Fig. 8 Magnetic hysteresis loops of **a** NiFe_2O_4 MNPs and **b** $\text{NiFe}_2\text{O}_4@\text{SiO}_2\text{-DETA@POM}$ particles

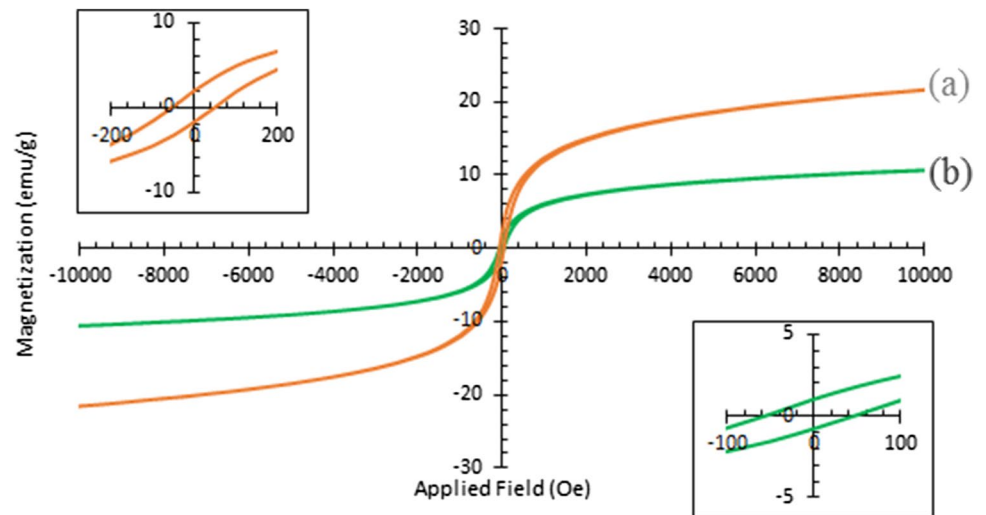


Fig. 9 TGA/DTG curve of NiFe₂O₄@SiO₂-DETA@POM particles

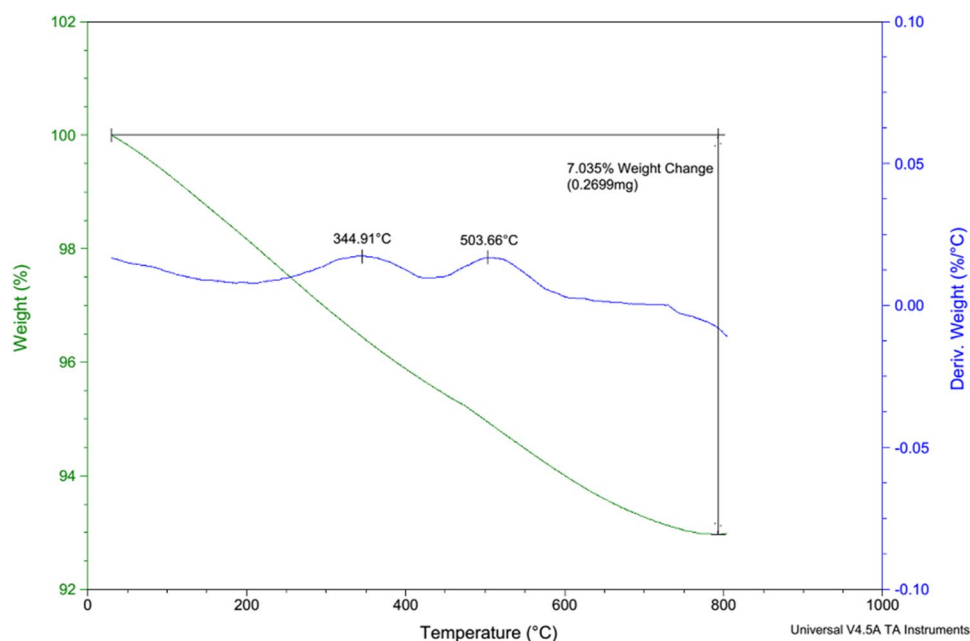


Table 1 Optimization of nano-NiFe₂O₄@SiO₂-DETA@POM catalyst and urea-hydrogen peroxide/acetic acid as oxidant in the ODS process

Entry	Nanocatalyst (g) ^a	Urea-hydrogen peroxide (g)	Acetic acid (mL)	ODS efficiency (%) ^b	
				BT	DBT
1	0.00	1	1	10	13
2	0.05	1	1	33	35
3	0.10	1	1	43	45
4	0.20	1	1	43	45
5	0.10	0.00	1	25	29
6	0.10	0.50	1	38	40
7	0.10	1.50	1	44	46
8	0.10	1	0	35	37
9	0.10	1	2	65	68
10	0.10	1	4	88	91
11	0.10	1	6	88	90

^aNiFe₂O₄@SiO₂-DETA@POM; ^bTemperature: 30 °C; time: 30 min

The effect of nanocatalyst and oxidant dosage on the ODS efficiency

At first, different amounts of the NiFe₂O₄@SiO₂-DETA@POM catalyst and urea-hydrogen peroxide/acetic acid as oxidant were determined for the ODS of HSCs present in model fuels with the concentration of 600 ppm at 30 °C in 30 min (Table 1). The effect of varying amounts of NiFe₂O₄@SiO₂-DETA@POM catalyst (0–0.20 g) on desulfurization efficiency was investigated in the presence of constant amounts of urea-hydrogen peroxide/acetic (1 g) and acetic acid (1 mL). According to Table 1, entry 1, in

the blank test (in the absence of a catalyst), only 10% of the BT and 13% of the DBT within 30 min were eliminated. As shown in Table 1, entry 3, for the optimal amount of nanocatalyst (0.1 g), 43% of the BT and 45% of the DBT removal were observed. Nevertheless, by increasing the amount of nanocatalyst to 0.2 g, no change in the sulfur removal was observed. The effect of various parameters on the ODS process is indicated in Table 1. Urea-hydrogen peroxide in the presence of an organic acid such as acetic acid was selected as an oxidizing agent. The results in Table 1, entry 10, confirm that the best sulfur removal percentage has occurred in the presence of 1 g of urea-hydrogen peroxide with 4 mL of acetic acid for DBT and BT compounds. By increasing the amount of the urea-hydrogen peroxide and acetic acid in sulfur removal, desulfurization efficiency increased rapidly from 0 g to 1 g for urea-hydrogen peroxide and 4 mL for acetic acid, and after that, no change has been observed. The literature survey revealed that in real gasoline, inorganic acids cannot dissolve; therefore, the sulfur removal percentage is lower than in organic acids (Rezvani et al. 2020b).

The effect of reaction temperature and time on the ODS efficiency

The two other influencing factors on the ODS efficiency of heterocyclic sulfur compounds (HSCs) are temperature and reaction time. The influence of temperature at 25, 30, 40, 50, and 60 °C and time 0 to 60 min on the desulfurization of sulfur compounds is demonstrated in Fig. 10a. As shown, the sulfur removal efficiency in HSCs increases with increasing the temperature from 25 to 50 °C in 30 min. However, increasing the temperature from 50 to

60 °C did not affect the oxidation efficiency. As shown in Fig. 10b, the ODS reaction was done at the optimum reaction temperature (50 °C) at various times. The best result occurred in 60 min for the desulfurization of HSCs. The oxidation reactivity was in the order of DBT > BT at the same temperature. The sulfur atom in BT has a lower electron density compared with DBT. So, the increase of the aromatic π -electron density has a positive effect on the oxidation efficiency of HSCs.

ODS process of real gas oil

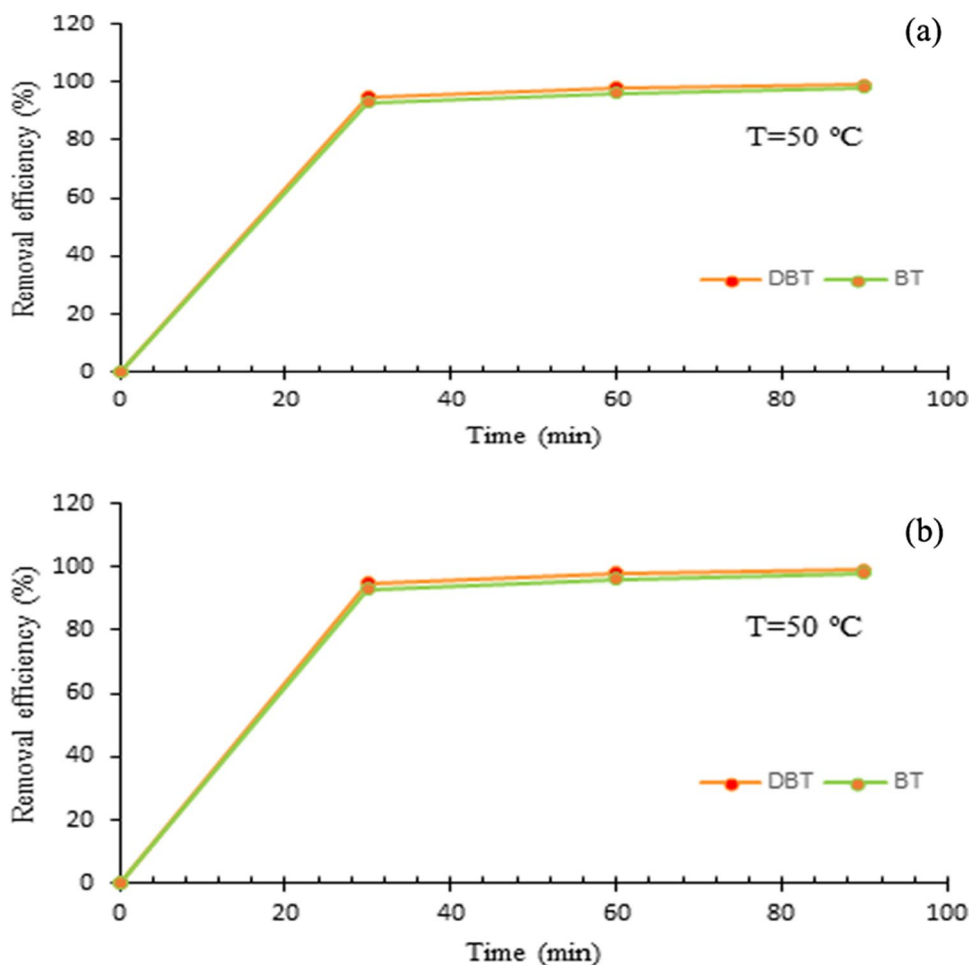
Gas oil and its products have different sulfur compounds, such as complex and linear compounds. In real samples, the variety and the high content of sulfur compounds make the desulfurization process more complicated. To evaluate the desulfurization process, a real sample of gas oil containing 600 ppm of sulfur was supplied by South Pars Company (Iran). Optimized reaction conditions (0.1 g of nano- $\text{NiFe}_2\text{O}_4@\text{SiO}_2\text{-DETA@POM}$ and 1 g/4 mL of urea hydrogen peroxide/acetic acid at 50 °C) were employed for ODS of a real gas oil sample. The excellent result of

96% removal of sulfur from the real gas oil was obtained in 60 min.

The proposed mechanism of the ODS process

A mechanism for the ODS process of HSCs in the presence of $\text{NiFe}_2\text{O}_4@\text{SiO}_2\text{-DETA@POM}$ nanocatalyst has been proposed in Scheme 2. The ODS process of the BT and DBT was done in n-heptane as a nonpolar oil phase. After that, the nanocatalyst and oxidant were added, and the oxidation reactions were performed in the nonpolar/catalyst interface phase. During the ODS process, the urea- H_2O_2 reacts with acetic acid (CH_3COOH) to in situ produce per-acetic acid ($\text{CH}_3\text{CO}_3\text{H}$). As one of the most considerable oxidizing systems, the catalytic sulfur oxidation mechanism is based on the peroxy-metal systems. The role of the metal atom (Mo) in the $\text{NiFe}_2\text{O}_4@\text{SiO}_2\text{-DETA@POM}$ nanocatalyst is to form peroxy-metal species that can convert organic sulfur to sulfones without forming residual products. The sulfur oxidation occurs via the electrophilic mechanism, so these electrophilic intermediate complex, MO_2 , were formed by the reaction of the peroxide oxygen in $\text{CH}_3\text{CO}_3\text{H}$ with

Fig. 10 The influence of temperature (a) and time (b) on the oxidation desulfurization process in the presence of $\text{NiFe}_2\text{O}_4@\text{SiO}_2\text{-DETA@POM}$



Scheme 2 Proposed mechanism for the oxidation desulfurization of gas oils in the presence of NiFe₂O₄@SiO₂-DETA@POM nanocatalyst using Urea-H₂O₂/acetic acid as an efficient oxidant

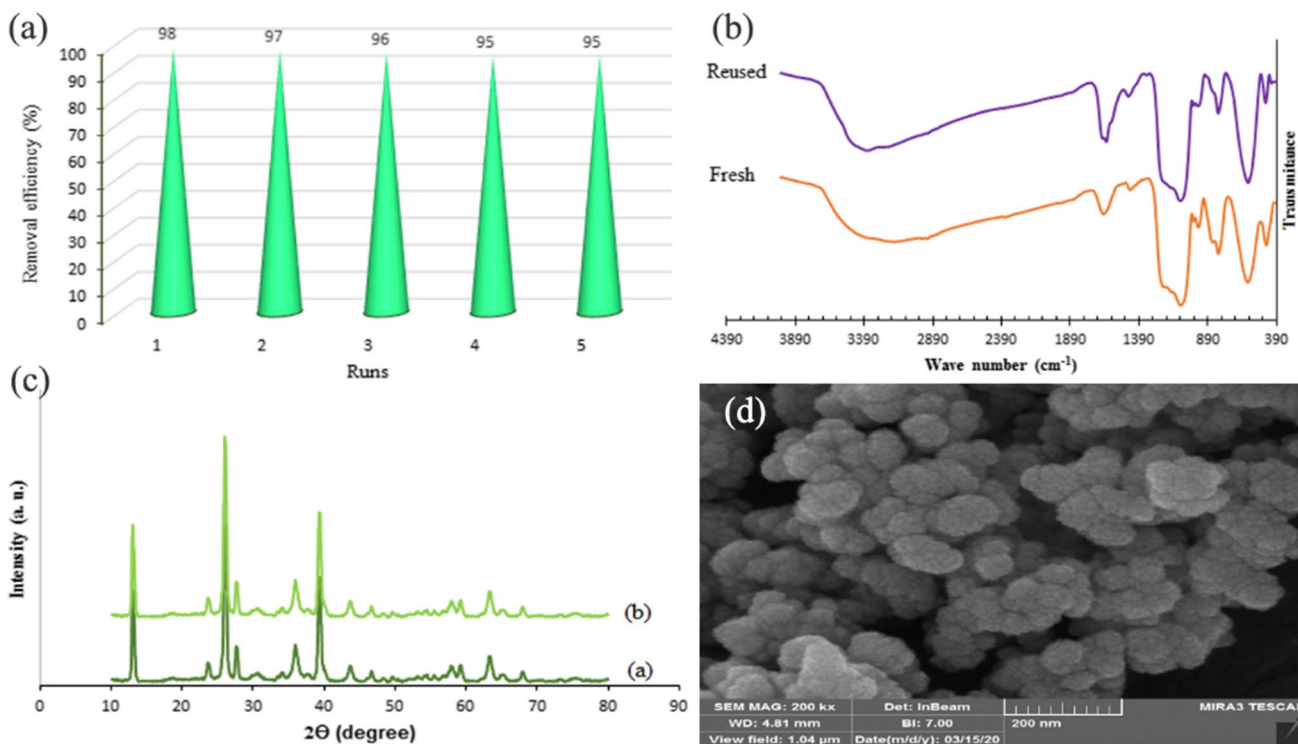
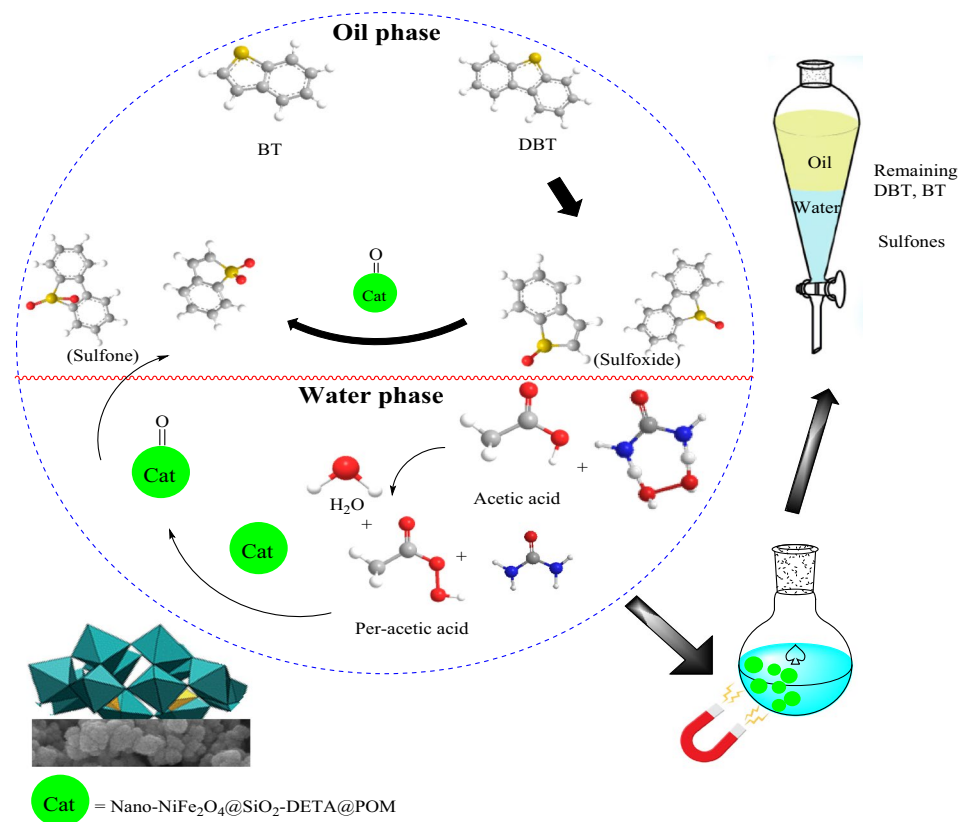


Fig. 11 **a** The recycling experiment diagram, **b** FT-IR spectrum, **c** XRD patterns, and **d** FE-SEM image of recycled NiFe₂O₄@SiO₂-DETA@POM catalyst after 5 runs

Table 2 Comparison of the catalytic activity of NiFe₂O₄@SiO₂-DETA@POM with other catalysts in the oxidative desulfurization removal of DBT from simulated fuels

No	Catalyst	Oxidant	Condition	Removal yield (%) ^b	Ref
1	rGO (5 mg)	O ₂ (200 mL/min)	140 °C, 6 h	91	Gu et al. 2017
2	([Omim][HSO ₄])SiO ₂ (50 mg)	H ₂ O ₂	50 °C, 50 min	98	Safa et al. 2017
3	PMo/BzPN-SiO ₂ (50 mg)	H ₂ O ₂	60 °C, 3 h	100	Craven et al. 2018
4	(PMnW ₁₁ @TiO ₂ @CS (10 mg)	CH ₃ COOH/H ₂ O ₂	35 °C, 1 h	98	Rezvani et al. 2018
5	(IL) ₃ PMo ₁₂ O ₄₀ /RS-MMS (10 mg)	H ₂ O ₂	60 °C, 50 min	98	Jiang et al. 2019
6	TBA-SiWMn@PVA (10 mg)	CH ₃ COOH/H ₂ O ₂	40 °C, 2 h	97	Rezvani et al. 2020b
7	POM-PGMA/SiO ₂ (30 mg)	H ₂ O ₂	25 °C, 2 h	97	Liu et al. 2020
8	NiFe ₂ O ₄ @SiO ₂ -DETA@POM (10 mg)	CH ₃ COOH/UHP	50 °C, 1 h	98	This work

terminal metal-oxygen groups (M=O_l) in the structure of sandwich-type POM.

Catalyst recovery and reusability

The reusability of nanocatalysts is a main parameter in evaluating their performance. To study the recoverability of the NiFe₂O₄@SiO₂-DETA@POM nanocatalyst for green chemistry view and commercial applications, at the end of the desulfurization process of real fuel, the nanocatalyst was separated by an external magnet, rinsed with ethanol, dried at 80 °C, and used again in the desulfurization process. The recycled nanocatalyst revealed the same catalytic performance without significant loss of activity after five runs (Fig. 11a). After the last run, the structural stability of the hybrid nanostructure was confirmed by the FT-IR spectrum (Fig. 11b), XRD patterns (Fig. 11c), and FE-SEM image (Fig. 11d).

A comparison of the performance of the prepared hybrid nanostructure (NiFe₂O₄@SiO₂-DETA@POM) and CH₃COOH/UHP oxidant system with other reported catalysts for the oxidative desulfurization of simulated fuels in literature is presented in Table 2. The presented data proves that NiFe₂O₄@SiO₂-DETA@POM is a suitable and efficient hybrid catalyst for the oxidative desulfurization of simulated and real fuels.

Conclusions

This research work was focused on the synthesis of magnetic hybrid nanomaterial (NiFe₂O₄@SiO₂-DETA@POM) as a new polyoxometalate-supported nanocatalyst in the presence of urea-H₂O₂/acetic acid as oxidant system to catalyze the oxidation-desulfurization reaction of the simulated and real gas oils. The sulfur-containing compounds were removed from simulated and real gas oils with high yields (96–98%). Moreover, this hybrid

nanomaterial showed good reusability after five oxidation runs with only a slight deterioration in its activity. Several key characteristics such as high performance, oxidant safety, easy work-up, eco-friendly process, and simple separation of catalyst by an external magnet provide new insights into the applications of polyoxometalate-decorated magnetic nanoparticles in the effective removal of organic sulfur from gas oil. Finally, we suggest the effectiveness of this nanostructure by variation in heteropolyacid structure or magnetic nanoparticles could be investigated in future works.

Author contribution M.A Bodaghifard conceived, planned, and supervised the project. P. Bayat carried out the experiments and analyses. M. Hamidinasab advised the project and wrote the manuscript with support from M.A. Bodaghifard. All authors discussed the results and contributed to the final manuscript. M.A. Bodaghifard revised the final version of the manuscript.

Funding The authors acknowledge the financial support of this work by the Research Council of Arak University.

Data availability There is no additional data.

Declarations

Ethical approval Not applicable.

Consent to participate Not applicable.

Consent for publication Not applicable.

Competing interests The authors declare no competing interests.

References

- Ammam M (2013) Polyoxometalates: formation, structures, principal properties, main deposition methods and application in sensing. *J Mater Chem A* 1:6291–6312. <https://doi.org/10.1039/C3TA01663C>

- Ahadi N, Bodaghifard MA, Mobinikhaledi A (2020) Preparation and characterization of a novel organic–inorganic hybrid nanostructure: application in synthesis of spirocompounds. *Res Chem Intermed* 46:3277–3294
- Bodaghifard MA, Hamidinasab M, Ahadi N (2018) Recent advances in the preparation and application of organic–inorganic hybrid magnetic nanocatalysts on multicomponent reactions. *Curr Org Chem* 22:234–267. <https://doi.org/10.2174/1385272821666170705144854>
- Bodaghifard MA, Shafi S (2021) Ionic liquid-immobilized hybrid nanomaterial: an efficient catalyst in the synthesis of benzimidazoles and benzothiazoles via anomeric-based oxidation. *J Iran Chem Soc* 18:677–687. <https://doi.org/10.1007/S13738-020-02055-1>
- Boniek D, Figueiredo D, Dos Santos AFB, De Resende Stoianoff MA (2015) Biodesulfurization: a mini review about the immediate search for the future technology. *Clean Technol Environ Policy* 17:29–37. <https://doi.org/10.1007/S10098-014-0812-X>
- Bodaghifard MA (2019) Palladium-melamine complex anchored on magnetic nanoparticles: a novel promoter for CC cross coupling reaction. *J Organomet Chem* 886:57–64. <https://doi.org/10.1016/j.jorganchem.2019.02.010>
- Chen TC, Shen YH, Lee WJ et al (2010) The study of ultrasound-assisted oxidative desulfurization process applied to the utilization of pyrolysis oil from waste tires. *J Clean Prod* 18:1850–1858. <https://doi.org/10.1016/J.JCLEPRO.2010.07.019>
- Cherevan AS, Nandan SP, Roger I et al (2020) Polyoxometalates on functional substrates: concepts, synergies, and future perspectives. *Adv Sci* 7:1903511. <https://doi.org/10.1002/ADVS.201903511>
- Craven M, Xiao D, Kunstmann-Olsen C et al (2018) Oxidative desulfurization of diesel fuel catalyzed by polyoxometalate immobilized on phosphazene-functionalized silica. *Appl Catal B* 231:82–91. <https://doi.org/10.1016/j.apcatb.2018.03.005>
- Gawande MB, Branco PS, Varma RS (2013) Nano-magnetite (Fe₃O₄) as a support for recyclable catalysts in the development of sustainable methodologies. *Chem Soc Rev* 42:3371–3393. <https://doi.org/10.1039/C3CS35480F>
- Gu Q, Wen G, Ding Y et al (2017) Reduced graphene oxide: a metal-free catalyst for aerobic oxidative desulfurization. *Green Chem* 19:1175–1181. <https://doi.org/10.1039/C6GC02894B>
- Hamidinasab M, Bodaghifard MA, Mobinikhaledi A (2020a) Green synthesis of 1H-pyrazolo[1,2-b]phthalazine-2-carbonitrile derivatives using a new bifunctional base–ionic liquid hybrid magnetic nanocatalyst. *Appl Organomet Chem* 34. <https://doi.org/10.1002/AOC.5386>
- Hamidinasab M, Bodaghifard MA, Mobinikhaledi A (2020b) Synthesis of new, vital and pharmacologically important bis phthalazine-triones using an efficient magnetic nanocatalyst and their HF and NBO investigation. *J Mol Struct* 1200:127091. <https://doi.org/10.1016/J.MOLSTRUC.2019.127091>
- HozhabrAraghi S, Entezari MH (2015) Amino-functionalized silica magnetite nanoparticles for the simultaneous removal of pollutants from aqueous solution. *Appl Surf Sci* 333:68–77. <https://doi.org/10.1016/j.apsusc.2015.01.211>
- Injumba W, Ritprajak P, Insin N (2017) Size-dependent cytotoxicity and inflammatory responses of PEGylated silica-iron oxide nanocomposite size series. *J Magn Magn Mater* 427:60–66. <https://doi.org/10.1016/j.jmmm.2016.11.015>
- Jiang W, Jia H, Fan X et al (2019) Ionic liquid immobilized on magnetic mesoporous microspheres with rough surface: application as recyclable amphiphilic catalysts for oxidative desulfurization. *Appl Surf Sci* 484:1027–1034. <https://doi.org/10.1016/j.apsusc.2019.03.341>
- Jiang W, Li H, Wang C et al (2016) Synthesis of ionic-liquid-based deep eutectic solvents for extractive desulfurization of fuel. *Energy Fuels* 30:8164–8170. https://doi.org/10.1021/ACS.ENERGYFUELS.6B01976/SUPPL_FILE/EF6B01976_SI_001.PDF
- Kim HS, Kim D, Kwak BS et al (2014) Synthesis of magnetically separable core at shell structured NiFe₂O₄ at TiO₂ nanomaterial and its use for photocatalytic hydrogen production by methanol/water splitting. *Chem Eng J* 243:272–279. <https://doi.org/10.1016/j.cej.2013.12.046>
- Liu Y, Zuo P, Wang R et al (2020) Covalent immobilization of Dawson polyoxometalates on hairy particles and its catalytic properties for the oxidation desulfurization of tetrahydrothiophene. *J Clean Prod* 274:122774. <https://doi.org/10.1016/j.jclepro.2020.122774>
- Nejati K, Zabihi R (2012) Preparation and magnetic properties of nano size nickel ferrite particles using hydrothermal method. *Chem Cent J* 6:1–6. <https://doi.org/10.1186/1752-153X-6-23/TABLES/2>
- Rezvani MA, Fereyduni M (2019) Synthesis of organic–inorganic hybrid nanocomposite polyoxometalate/metal oxide/CS polymer (PMnW11@TiO₂@CS): nanocatalyst for oxidative desulfurization of real fuel. *ChemistrySelect* 4:11467–11474. <https://doi.org/10.1002/SLCT.201902654>
- Rezvani MA, Hadi M, Mirsadri SA (2020a) Synthesis of new nanocomposite based on nanoceramic and mono substituted polyoxometalate, PMo11Cd@MnFe₂O₄, with superior catalytic activity for oxidative desulfurization of real fuel. *Appl Organomet Chem* 34:e5882. <https://doi.org/10.1002/AOC.5882>
- Rezvani MA, Shaterian M, Aghmasheh M (2020b) Catalytic oxidative desulfurization of gasoline using amphiphilic polyoxometalate@polymer nanocomposite as an efficient, reusable, and green organic–inorganic hybrid catalyst. *Environ Technol* 41:1219–1231. <https://doi.org/10.1080/09593330.2018.1526217>
- Rezvani MA, Imani A (2021) Ultra-deep oxidative desulfurization of real fuels by sandwich-type polyoxometalate immobilized on copper ferrite nanoparticles, Fe₆W₁₈O₇₀CuFe₂O₄, as an efficient heterogeneous nanocatalyst. *J Environ Chem Eng* 9. <https://doi.org/10.1016/j.jece.2020.105009>
- Rezvani MA, Mirsadri SA (2020) Synthesis and characterization of new hybrid inorganic–organic polymer nanocomposite as efficient catalyst for oxidative desulfurization of real fuel. *Appl Organomet Chem* 34:e5585. <https://doi.org/10.1002/AOC.5585>
- Rezvani MA, Shaterian M, Akbarzadeh F, Khandan S (2018) Deep oxidative desulfurization of gasoline induced by PMoCu@MgCu₂O₄-PVA composite as a high-performance heterogeneous nanocatalyst. *Chem Eng J* 333:537–544. <https://doi.org/10.1016/J.CEJ.2017.09.184>
- Safa M, Mokhtarani B, Mortaheb HR et al (2017) Oxidative desulfurization of diesel fuel using a brønsted acidic ionic liquid supported on silica gel. *Energy Fuels* 31:10196–10205. <https://doi.org/10.1021/ACS.ENERGYFUELS.6B03505>
- Sen R, Jain P, Patidar R et al (2015) Synthesis and characterization of nickel ferrite (NiFe₂O₄) nanoparticles prepared by sol-gel method. *Mater Today: Proceedings* 2:3750–3757. <https://doi.org/10.1016/j.matpr.2015.07.165>
- Taghizadeh M, Mehrvarz E, Taghipour A (2020) Polyoxometalate as an effective catalyst for the oxidative desulfurization of liquid fuels: a critical review. *Rev Chem Eng* 36:831–858. <https://doi.org/10.1515/REVCE-2018-0058/XML>
- Yang E, Yao C, Liu Y et al (2018) Bamboo-derived porous biochar for efficient adsorption removal of dibenzothiophene from

model fuel. *Fuel* 211:121–129. <https://doi.org/10.1016/j.fuel.2017.07.099>

Ye JJ, De Wu C (2016) Immobilization of polyoxometalates in crystalline solids for highly efficient heterogeneous catalysis. *Dalton Trans* 45:10101–10112. <https://doi.org/10.1039/C6DT01378C>

Zhou Y, Chen G, Long Z, Wang J (2014) Recent advances in polyoxometalate-based heterogeneous catalytic materials for liquid-phase organic transformations. *RSC Adv* 4:42092–42113. <https://doi.org/10.1039/C4RA05175K>

Publisher's note Springer Nature remains neutral with regard to jurisdictional claims in published maps and institutional affiliations.

Springer Nature or its licensor (e.g. a society or other partner) holds exclusive rights to this article under a publishing agreement with the author(s) or other rightsholder(s); author self-archiving of the accepted manuscript version of this article is solely governed by the terms of such publishing agreement and applicable law.